Search for $K^0_{S(L)} \to \pi^+\pi^-\mu^+\mu^-$ decays at LHCb

R. Aaij *et al.*[*]
(LHCb Collaboration)

(Received 12 November 2025; accepted 13 February 2026; published 2 April 2026)

A search for $K^0_{S(L)} \to \pi^+\pi^-\mu^+\mu^-$ decays is performed using proton-proton collision data collected by the LHCb experiment at a center-of-mass energy of 13 TeV, corresponding to an integrated luminosity of 5.4 fb^{-1}. No $K^0_{S(L)} \to \pi^+\pi^-\mu^+\mu^-$ signals are found and upper limits are set for the first time on the branching fractions $\mathcal{B}(K^0_S \to \pi^+\pi^-\mu^+\mu^-) < 1.4 \times 10^{-9}$ and $\mathcal{B}(K^0_L \to \pi^+\pi^-\mu^+\mu^-) < 6.6 \times 10^{-7}$, at the 90% confidence level.

DOI: 10.1103/s1dv-cv1t

I. INTRODUCTION

Radiative decays of neutral kaons, in which a virtual photon converts into a Dalitz pair of leptons, provide a powerful laboratory for testing chiral perturbation theories and studying *CP* violation [1]. In particular, the $K^0 \to \pi^+\pi^-\gamma^*$, with $\gamma^* \to \ell\ell$, decay proceeds through two different processes: inner bremsstrahlung, in which the virtual photon is emitted from the external charged pions, and direct emission, where the photon is generated at the weak vertex (Fig. 1). The *CP* information is encoded in the photon polarization and, equivalently, in the distribution of the angle between the dipion and dilepton planes [2]. As the K^0_L and K^0_S mesons have opposite *CP* eigenvalues, the $K^0_L \to \pi^+\pi^-\gamma^*$ and $K^0_S \to \pi^+\pi^-\gamma^*$ decays provide complementary constraints. The short-lived mode is dominated by the $K^0_S \to \pi^+\pi^-$ process with inner bremsstrahlung and gives access to the long-distance (LD) chiral terms, while the long-lived mode is dominated by the direct emission (as the $K^0_L \to \pi^+\pi^-$ decay is heavily suppressed) and grants access to *CP*-violating terms [2].

Dalitz decays of the electron modes, $K^0_{S(L)} \to \pi^+\pi^-e^+e^-$, have been observed by KTeV [3] and KEK [4] Collaborations. The most recent and precise results are provided by NA48 collaboration. Their branching fractions $\mathcal{B}(K^0_L \to \pi^+\pi^-e^+e^-) = (3.08 \pm 0.09 \pm 0.18) \times 10^{-7}$, and $\mathcal{B}(K^0_S \to \pi^+\pi^-e^+e^-) = (4.83 \pm 0.11 \pm 0.14) \times 10^{-5}$ [5,6], differ by 2 orders of magnitude, as expected due to the opposite *CP* eigenvalues [2,7].

The equivalent muonic mode, $K^0_{S(L)} \to \pi^+\pi^-\mu^+\mu^-$, probes higher values of lepton-pair invariant mass (q), and thus has larger sensitivity to *CP*-violating observables where the direct emission contribution is enhanced with respect to the electron mode. The $K^0_{S(L)} \to \pi^+\pi^-\mu^+\mu^-$ decay is highly suppressed in the standard model due to the phase-space limitations presented by the $\sim 7\ \text{MeV}/c^2$ difference in mass between the parent $K^0_{S(L)}$ and the four final-state particles. Theoretical calculations of $\mathcal{B}(K^0_S \to \pi^+\pi^-\mu^+\mu^-)$ are dominated by LD contributions to the $K^0_S \to \pi^+\pi^-\gamma^*$ decay, and give $\mathcal{B}(K^0_S \to \pi^+\pi^-\mu^+\mu^-) = (417.00 + 2.17 + 49.80) \times 10^{-16}$ [1], where the first term is due to a bremsstrahlung photon emitted by the pion, the second term accounts for the direct emission of the photon at the weak vertex, and the last term represents their interference. Theoretical calculations for $\mathcal{B}(K^0_L \to \pi^+\pi^-\ell^+\ell^-)$ have been performed in Refs. [2,7,8] for $\ell = e$, but no specific prediction is given for $\mathcal{B}(K^0_L \to \pi^+\pi^-\mu^+\mu^-)$. Experimentally, neither the $K^0_S \to \pi^+\pi^-\mu^+\mu^-$ nor the $K^0_L \to \pi^+\pi^-\mu^+\mu^-$ decays have been searched for before.

The LHCb experiment [9] has proven its strong capabilities to study rare kaon decays thanks to its excellent tracking and particle identification (PID) performance, versatile trigger system, and large hadron production rate. LHCb collaboration has previously set world-best upper limits on $\mathcal{B}(K^0_S \to \mu^+\mu^-)$ [10] and $\mathcal{B}(K^0_{S(L)} \to \mu^+\mu^-\mu^+\mu^-)$ [11].

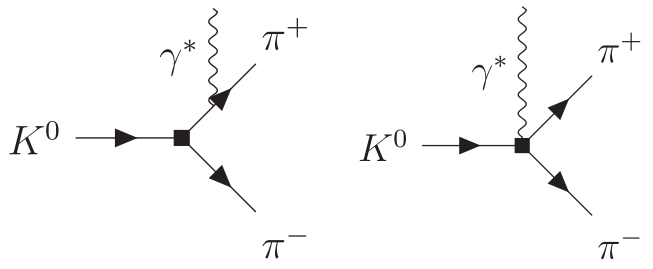

FIG. 1. Tree-level diagrams in chiral perturbation theory for the $K^0 \to \pi^+\pi^-\gamma^*$ decay with (left) inner bremsstrahlung and (right) direct emission of a γ^* photon.

[*]Full author list given at the end of the article.

This paper presents the first-ever search for $K^0_{S(L)} \to \pi^+\pi^-\mu^+\mu^-$, using proton-proton ($pp$) collision data collected by the LHCb experiment during 2016–2018 at a center-of-mass energy of 13 TeV, and corresponding to an integrated luminosity of 5.4 fb^{-1}.

II. ANALYSIS STRATEGY

The branching fractions are measured with respect to the $K^0_S \to \pi^+\pi^-$ decay, according to

$$\mathcal{B}(K^0_{S(L)} \to \pi^+\pi^-\mu^+\mu^-) = \alpha_{S(L)} N_{\pi^+\pi^-\mu^+\mu^-}, \quad (1)$$

where the normalization factor $\alpha_{S(L)}$, also known as single-event sensitivity,[1] is defined as

$$\alpha_{S(L)} \equiv \mathcal{B}(K^0_S \to \pi^+\pi^-) \frac{\varepsilon_{K^0_S \to \pi^+\pi^-}}{N_{\pi^+\pi^-} \varepsilon_{K^0_{S(L)} \to \pi^+\pi^-\mu^+\mu^-}}. \quad (2)$$

The parameter $\varepsilon_{K^0_S \to \pi^+\pi^-}$ ($\varepsilon_{K^0_{S(L)} \to \pi^+\pi^-\mu^+\mu^-}$) represents the product of the reconstruction, trigger, and selection efficiency of $K^0_S \to \pi^+\pi^-$ ($K^0_{S(L)} \to \pi^+\pi^-\mu^+\mu^-$) candidates. The observed number of $K^0_{S(L)} \to \pi^+\pi^-\mu^+\mu^-$ candidates is $N_{\pi^+\pi^-\mu^+\mu^-}$, the observed number of $K^0_S \to \pi^+\pi^-$ candidates is $N_{\pi^+\pi^-}$, and $\mathcal{B}(K^0_S \to \pi^+\pi^-) = (69.20 \pm 0.05)\%$ [12] is the branching fraction of the normalization channel. The $K^0_S \to \pi^+\pi^-$ normalization channel is selected due to its abundant rate. Furthermore, it enables cancellation of the K^0 production rate and reduces systematic uncertainties related to final-state particle reconstruction.

At LHCb, the $K^0_L \to \pi^+\pi^-\mu^+\mu^-$ and $K^0_S \to \pi^+\pi^-\mu^+\mu^-$ decays are indistinguishable on an event-by-event basis [9]. For this reason, the K^0_L contribution is not considered when setting the upper limit for $K^0_S \to \pi^+\pi^-\mu^+\mu^-$, and vice versa. As a consequence, the set upper limits are more conservative than they would be if the K^0_S and K^0_L modes could be distinguished. The LHCb acceptance for K^0_L decays is $\sim 2 \times 10^{-3}$ times that of the K^0_S modes [9]. The only relevant difference between $K^0_S \to \pi^+\pi^-\mu^+\mu^-$ and $K^0_L \to \pi^+\pi^-\mu^+\mu^-$ at the reconstruction level is the lifetime. As a consequence, the selection strategy is optimized for $K^0_S \to \pi^+\pi^-\mu^+\mu^-$ decays and then applied to $K^0_L \to \pi^+\pi^-\mu^+\mu^-$ decays. The K^0_S–K^0_L interference is ignored, as K^0 and $\bar{K}^0$ mesons are produced in similar amounts at LHC [13].

III. LHCB DETECTOR AND TRIGGER

The LHCb detector [14,15] is a single-arm forward spectrometer covering the pseudorapidity range $2 < \eta < 5$, designed for the study of particles containing b or c quarks. The detector used for this analysis includes a high-precision tracking system consisting of a silicon-strip vertex detector (VELO) surrounding the pp interaction region [16], a large-area silicon-strip detector located upstream of a dipole magnet with a bending power of about 4 T m, and three stations of silicon-strip detectors and straw drift tubes [17] placed downstream of the magnet. The tracking system provides a measurement of the momentum (p) of charged particles with a relative uncertainty that varies from 0.5% at low momentum to 1.0% at 200 GeV/c. The minimum distance of a track to a pp collision vertex (PV), the impact parameter (IP), is measured with a resolution of $(15 + 29/p_T)$ μm, where p_T is the component of the momentum transverse to the beam axis, in GeV/c. Different types of charged hadrons are distinguished using information from two ring-imaging Cherenkov (RICH) detectors [18]. Photons, electrons, and hadrons are identified by a calorimeter system consisting of scintillating pad and preshower detectors, and an electromagnetic and a hadronic calorimeter. Muons are identified by a system composed of alternating layers of iron and multiwire proportional chambers [19]. In addition, information from the tracking system, the calorimeter system, and the RICH detectors is used to further improve the muon identification.

Events are first filtered by a hardware trigger, known as L0 [20], which uses information from the calorimeter and the muon system to select muon candidates with p_T above a few GeV/c. Subsequently, a full event reconstruction is applied in the high-level trigger (HLT), which is subdivided into two steps, HLT1 and HLT2. The HLT1 algorithms for strange decays were improved in 2016 [21,22], boosting the efficiency of the $K^0_S \to \pi^+\pi^-\mu^+\mu^-$ channel, amongst others. For this reason, only the 2016–2018 data are considered in this measurement. In the off-line selection, trigger signals are associated with reconstructed particles. Selection requirements can therefore be made on the trigger selection itself and on whether the decision was due to the signal candidate (trigger on signal, TOS) or other particles produced in the pp collision (trigger independent of signal, TIS). To enhance the L0 trigger efficiency, events fulfilling either the TIS or TOS requirements are considered in this analysis. The $K^0_S \to \pi^+\pi^-$ normalization channel candidates are reconstructed from data selected by a trigger line requiring only the presence of a pp interaction, providing an unbiased representation of the collision. The triggered data further undergo a centralized, off-line processing step [23].

Simulation is used to model the effects of the detector acceptance and selection requirements. In the simulation, pp collisions are generated using PYTHIA 8 [24,25] with a specific LHCb configuration [26]. Decays of unstable particles are described by EvtGen [27], in which final-state radiation is generated using PHOTOS [28]. The interaction of

[1]The value of $\mathcal{B}(K^0_S \to \pi^+\pi^-\mu^+\mu^-)$ corresponding to one signal event seen in the data sample.

the generated particles with the detector, and its response, are implemented using the Geant4 toolkit [29,30], as described in Ref. [31]. The simulated samples are corrected to account for known data simulation differences in the K^0_S production kinematics, as well as the track reconstruction and PID efficiencies. The analysis strategy is developed using $K^0_S \to \pi^+\pi^-\mu^+\mu^-$ simulated samples. Given the K^0_L decay only differs due to its lifetime, the $K^0_L \to \pi^+\pi^-\mu^+\mu^-$ efficiency is obtained by weighting the decay time distribution of the simulated $K^0_S \to \pi^+\pi^-\mu^+\mu^-$ sample to match that of the K^0_L meson.

IV. SIGNAL SELECTION

This measurement benefits from the large kaon production cross section at the LHC, approximately 0.3 b for both K^0_S and K^0_L mesons [9], as well as from the forward production of kaons, which fall within the LHCb detector acceptance. The K^0_S candidates from both the signal and the normalization channels are required to originate from a PV. In case of multiple choices, the PV that fits best to the flight direction of the K^0_S candidate is chosen as the associated PV. Candidate $K^0_S \to \pi^+\pi^-\mu^+\mu^-$ decays are reconstructed by combining pairs of oppositely charged, well-identified muons and pions originating from a common vertex, displaced from the PV. Candidates with an invariant mass in the region $490 < m(\pi^+\pi^-\mu^+\mu^-) < 600$ MeV$/c^2$ are retained for further analysis. In order to avoid experimenter's bias, selected candidates in the region $490 < m(\pi^+\pi^-\mu^+\mu^-) < 510$ MeV$/c^2$, which contains approximately 97% of the signal, were removed from the data sample until the analysis procedure had been finalized.

Given the relatively long lifetime of the K^0_S meson, only about one-third of its decays occur inside the VELO, while the remainder take place downstream in the detector. Decays inside the VELO can be reconstructed with an invariant-mass resolution roughly twice as good as those outside. Moreover, the online event selection relies on tracks with hits in both the VELO and the downstream tracking stations. Consequently, only decays taking place inside the VELO are retained in this analysis.

Several selections are applied to reconstructed candidates in order to further reduce background contributions. These include requirements on the maximum distance of closest approach between any pair of the four signal tracks, the flight distance from the PV of the K^0_S candidate on the plane transverse to the beam direction, the angles between the two muon and the two pion tracks, and PID variables of the final-state pions and muons.

The only non-negligible background source in the signal channel arises from random combinations of tracks, which originate from a pp interaction region or from inelastic interactions of the products of the pp collision with the detector material. A boosted decision tree (BDT) [32,33] classifier implemented in the XGBoost package [34] is used to further separate the signal from the combinatorial background. One BDT per trigger category (TIS and TOS) is used, each including as discriminating variables:

(i) the significance of the distance between the candidate decay vertex and any element of the VELO material [35];
(ii) the smallest IP value of each of the muon and pion candidates with respect to any of the PVs reconstructed in the event;
(iii) the smallest IP value of the K^0_S candidate to any of the PVs reconstructed in the event;
(iv) the difference in χ^2 of the PV fit when the K^0_S candidate is or is not included;
(v) the transverse displacement of the K^0_S decay vertex from the beam line; and
(vi) the maximum distance of closest approach between any pair of the four final-state tracks.

The BDT is trained with simulated $K^0_S \to \pi^+\pi^-\mu^+\mu^-$ decays as a proxy for the signal, and $\pi^+\pi^-\,\mu^+\mu^-$ combinations with an invariant mass $m(\pi^+\pi^-\mu^+\mu^-) > 510$ MeV$/c^2$ as a proxy for the background. To mitigate the effects of statistical fluctuations and minimize overtraining, the k-fold method [36], with $k = 6$, is used during the training.

The BDT requirement is optimized for the best expected upper limit at the 90% confidence level (CL) using pseudoexperiments, performing fits as explained below. The BDT requirement corresponds to a signal efficiency of approximately 80% (95%) for the TIS (TOS) sample, and a background suppression above 99.9%. After the BDT selection requirement, in the case of multiple candidates per event, a single candidate is chosen arbitrarily.

V. FIT MODEL AND NORMALIZATION DECAY MODE

The signal yield $N_{\pi^+\pi^-\mu^+\mu^-}$ is obtained from a simultaneous, extended unbinned maximum-likelihood fit to the four-track invariant-mass distributions of the signal candidates in the two trigger categories. The invariant-mass distributions of the selected candidate events, and the result of the described mass fit, are shown in Fig. 2. No physical candidates with an invariant mass lower than 490 MeV$/c^2$ can exist due to conservation of energy. To account for this, the invariant-mass distribution of the background follows the distribution of the available momentum in a two-body $K^0_S \to (\pi^+\pi^-)(\mu^+\mu^-)$ decay. This distribution is modeled by a function with only one free parameter, which dictates the kinematic threshold of the candidates,

$$Q(m, A) = \begin{cases} \sqrt{\Delta} & \text{if } \Delta > 0 \\ 0 & \text{if } \Delta < 0 \end{cases}, \tag{3}$$

with

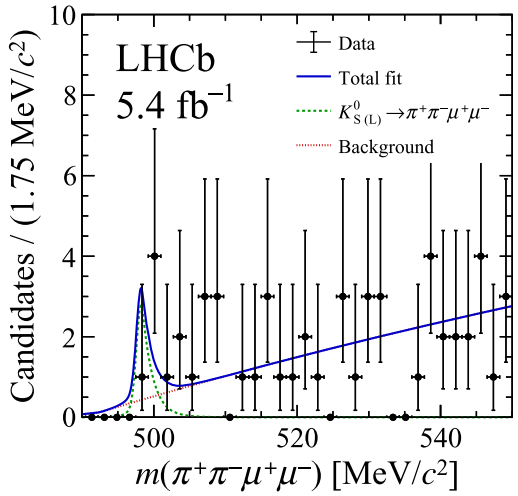

FIG. 2. Invariant-mass distribution of selected $K^0_{S(L)} \to \pi^+\pi^-\mu^+\mu^-$ candidates in the TIS and TOS trigger categories combined. The blue lines show the result of a simultaneous fit to both categories.

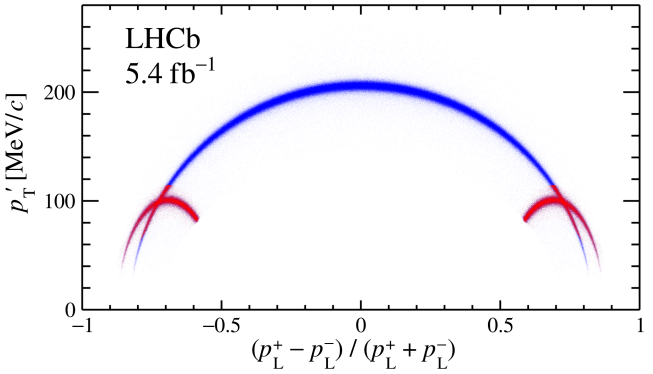

FIG. 3. Distribution of selected $K^0_S \to \pi^+\pi^-$ candidates in data in the Armenteros-Podolanski plane. The variables of the plane are the longitudinal momentum asymmetry between the positively (p_L^+) and negatively (p_L^-) charged pions, and the transverse momentum of the pions with respect to the K^0_S flight direction, p'_T. The blue region, containing $K^0_S \to \pi^+\pi^-$ decays, is accepted, while the red regions, containing background from $\Lambda \to p\pi^-$ and $\bar{\Lambda} \to \bar{p}\pi^+$ decays, are rejected.

$$\Delta = \frac{[(m-A)^2 - (2m_\mu + 2m_\pi)^2][(m-A)^2 - (2m_\mu - 2m_\pi)^2]}{4(m-A)^2}, \tag{4}$$

where m is the four-track invariant mass $m(\pi^+\pi^-\mu^+\mu^-)$, and A is its minimum value, which can exceed the sum of the masses of the two pions and two muons due to the requirements on the minimum angle between the decay products. Specifically, Q is the center-of-mass momentum in a two-body decay, introducing an offset, A, on the mass of the origin particle, m, that models the kinematic threshold for the detector. The A parameter is extracted from the fit. The background model is validated on background-enriched data obtained by loosening the BDT selection requirement. The $K^0_S \to \pi^+\pi^-\mu^+\mu^-$ signal invariant-mass shape is parametrized by the sum of two Crystal Ball functions [37], with the same peak position, and power-law tails on opposite sides of the distribution. The parameter values of the signal distribution are obtained from simulated events with corrections obtained from a fit of $K^0_S \to \pi^+\pi^-$ decays in data, following Ref. [10].

The $K^0_S \to \pi^+\pi^-$ candidates, selected by combining two well-identified pions with opposite charge originating from a common vertex, are further restricted to specific regions of the Armenteros-Podolanski plane [38] in order to suppress contributions from $\Lambda \to p\pi^-$ and $\bar{\Lambda} \to \bar{p}\pi^+$ decays, as seen in Fig. 3. The details of the selection used can be found in the Appendix. The $N_{\pi^+\pi^-}$ value is determined as the number of candidates in the mass range $400 < m(\pi^+\pi^-) < 600$ MeV/c^2. Due to the negligible background contribution after the selection in the $K^0_S \to \pi^+\pi^-$ sample, as illustrated by Fig. 4, no fit to the invariant-mass distribution is performed to determine the number of $K^0_S \to \pi^+\pi^-$ decays.

The efficiencies are assumed to factorize according to

$$\varepsilon = \varepsilon^{\text{reco}}\varepsilon^{\text{sel/reco}}\varepsilon^{\text{trig/sel}}. \tag{5}$$

Here, $\varepsilon^{\text{reco}}$ is the reconstruction efficiency, $\varepsilon^{\text{sel/reco}}$ is the selection efficiency for the reconstructed signal candidates, and $\varepsilon^{\text{trig/sel}}$ is the trigger efficiency for selected candidates. The $\varepsilon^{\text{reco}}$ efficiency includes track and vertex reconstruction effects and is estimated from simulation to be ∼0.2% for $K^0_S \to \pi^+\pi^-\mu^+\mu^-$ decays and ∼1.5% for $K^0_S \to \pi^+\pi^-$ decays. The $\varepsilon^{\text{sel/reco}}$ efficiency, for $K^0_S \to \pi^+\pi^-\mu^+\mu^-$ decays, includes the BDT and PID requirements and is estimated to be around 7%. The equivalent efficiency for $K^0_S \to \pi^+\pi^-$ decays includes the cut on the Armenteros-Podolanski plane, and it is approximately 46%. Lastly, the $\varepsilon^{\text{trig/sel}}$ efficiency is determined to be around 1% for $K^0_S \to \pi^+\pi^-\mu^+\mu^-$ decays. The unbiased trigger selection used for the $K^0_S \to \pi^+\pi^-$ mode is too loose to record every selected event. The acceptance rate is artificially reduced by considering only one event in every 10^{-7} collision. This is considered as trigger efficiency for the $K^0_S \to \pi^+\pi^-$ mode. The efficiencies are calculated using simulation samples with corrections derived from $K^0_S \to \pi^+\pi^-$ decays in data. The tracking efficiency is obtained using dedicated control samples of $J/\psi \to \mu^+\mu^-$ and $K^0_S \to \pi^+\pi^-$ decays using a tag-and-probe method [39]. Similarly, PID efficiencies are obtained using calibration samples of low-momentum muons from $J/\psi \to \mu^+\mu^-$ decays collected concurrently

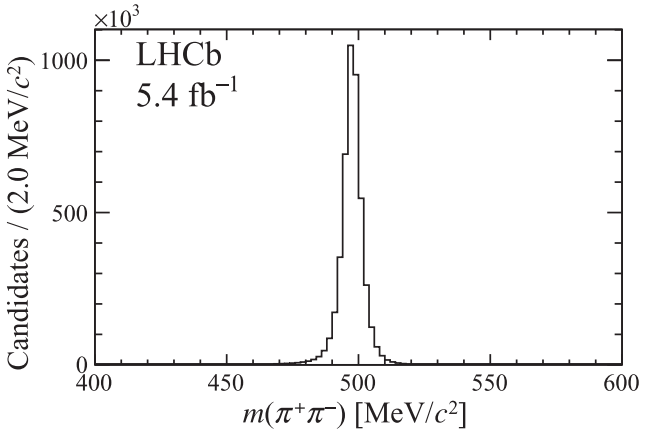

FIG. 4. Invariant-mass distribution of the selected $K^0_S \to \pi^+\pi^-$ candidates.

with the data used for the analysis. The relatively low selection efficiency for the $K^0_S \to \pi^+\pi^-\mu^+\mu^-$ channel is primarily driven by the limited phase space available, the small mass difference between the K^0_S and the four final-state particles results in low-p_T final-state products and small opening angles. This makes it difficult to distinguish signal tracks from the background produced in pp collisions without a significant loss in efficiency. The trigger efficiencies obtained in simulation are validated with $K^0 \to \pi^\pm\mu^\mp\overset{(-)}{\nu}_\mu$ decays, by comparing the trigger efficiency in simulation and data, as described in Ref. [10]. The simulated samples used to compute the efficiencies are generated assuming the decay amplitude is uniform over the phase space of the K^0_S particle without accounting for the presence of any intermediate resonances. The obtained efficiencies are verified to be independent of such effects. The efficiency for the $K^0_L \to \pi^+\pi^-\mu^+\mu^-$ decay is derived using the same procedure applied to $K^0_S \to \pi^+\pi^-\mu^+\mu^-$ simulated samples, weighted to reproduce the K^0_L lifetime, as mentioned in Sec. III.

VI. SYSTEMATIC UNCERTAINTIES

Table I shows the sources of systematic uncertainty on α_S considered in this analysis. The systematic uncertainties are incorporated into the fit of the signal-candidate mass distribution as Gaussian priors on the single event sensitivity. For convenience, sources of systematic uncertainty are separated into those acting independently on each trigger category and those affecting the overall normalization factor.

A 1% systematic uncertainty on the efficiencies accounts for minor modifications of the trigger selection criteria throughout the Run 2 data-taking period. These are determined by comparing the yields of triggered $K^0 \to \pi^\pm\mu^\mp\overset{(-)}{\nu}_\mu$ and $K^0_S \to \pi^+\pi^-$ decays from the trigger-unbiased data. To compute the systematic uncertainty associated with the corrections applied to the simulation, the efficiency ratio is recomputed with and without corrections on the kaon momenta. Half of the correction is taken as the systematic uncertainty and amounts to a 9% effect on $\alpha_{S(L)}$. The systematic uncertainty on the $K^0_S \to \pi^+\pi^-$ yield is evaluated by comparing the number of selected $K^0_S \to \pi^+\pi^-$ candidates in data with the yield obtained from a fit to the $\pi^+\pi^-$ invariant mass with a floating background component modeled as an exponential function. A 1% systematic uncertainty contribution is found to cover any variation. The uncertainty on the PID efficiency corrections is propagated to the ratio of efficiencies and gives an additional 2% systematic uncertainty. The differences between data and simulation in the track reconstruction efficiencies, determined using control channels from data, are covered by a 2% systematic uncertainty. The L0 and HLT efficiencies for the $K^0_S \to \pi^+\pi^-\mu^+\mu^-$ signal are determined using $K^0 \to \pi^\pm\mu^\mp\overset{(-)}{\nu}_\mu$ decays as control modes. The efficiencies are found to be compatible between data and simulation, and their difference is used as the systematic uncertainty, following Ref. [10]. The $K^0 \to \pi^\pm\mu^\mp\overset{(-)}{\nu}_\mu$ sample at LHCb is composed of K^0_S and K^0_L in similar amounts, due to a compensation between the different branching fractions [40–42], and the different reconstruction efficiency driven by the decay-time acceptance, which produces similar decay-time distributions for reconstructed K^0_L and K^0_S decays. A systematic uncertainty of 1.4% is added to the relative efficiency between $K^0_S \to \pi^+\pi^-\mu^+\mu^-$ and $K^0_L \to \pi^+\pi^-\mu^+\mu^-$ decays, when measuring $\mathcal{B}(K^0_L \to \pi^+\pi^-\mu^+\mu^-)$. This systematic uncertainty covers the difference of the efficiency ratio across the data-taking period as well as uncertainties related to the limited simulation sample size. The systematic uncertainties from the signal and background invariant-mass models are negligible at the current level of precision. The uncertainty on the branching fraction $\mathcal{B}(K^0_S \to \pi^+\pi^-) = (69.20 \pm 0.05)\%$ induces a 0.07% uncertainty on $\alpha_{S(L)}$, also considered negligible.

TABLE I. Summary of the sources of systematic uncertainty, as well as their relative effect on the single event sensitivity, α_S.

Source	Relative effect (%)
Variations in data taking	1
Data/simulation differences	9
$K^0_S \to \pi^+\pi^-$ yield	1
PID	2
Tracking	2
L0	9 (TIS), 11 (TOS)
HLT	13
Total	18 (TIS), 19 (TOS)

VII. RESULTS AND CONCLUSIONS

The number of trigger efficiency–corrected $K^0_S \to \pi^+\pi^-$ decays is found to be $(8.79 \pm 0.11) \times 10^{12}$. The efficiency ratios, $\varepsilon_{K^0_S\to\pi^+\pi^-}/\varepsilon_{K^0_S\to\pi^+\pi^-\mu^+\mu^-}$, are determined to be $(2.9 \pm 0.3) \times 10^3$ and $(5.4 \pm 0.5) \times 10^3$ for the TIS and TOS categories, respectively. Note that the trigger efficiency is considered in the $K^0_S \to \pi^+\pi^-$ yield instead of on the efficiency ratios. The obtained normalization factors are $\alpha_S^{\mathrm{TIS}} = (2.27 \pm 0.42) \times 10^{-10}$ and $\alpha_S^{\mathrm{TOS}} = (4.21 \pm 0.81) \times 10^{-10}$, assuming that the muons and pions are uniformly distributed in phase space for $K^0_S \to \pi^+\pi^-\mu^+\mu^-$ decays. The normalization factors, α_{TIS} and α_{TOS}, are derived for the $K^0_L \to \pi^+\pi^-\mu^+\mu^-$ decay, using Eq. (2), and the efficiency for $K^0_L \to \pi^+\pi^-\mu^+\mu^-$ decays, computed as described in Sec. V.

The final data are consistent with the background-only hypothesis at the level of 1.9 standard deviations, showing no evidence for a signal. Upper limits are set, at 90% CL, by integrating the exponent of the negative profiled log-likelihood up to 90% of its total area, validated using pseudoexperiments. The upper limits are determined to be

$$\mathcal{B}(K^0_S \to \pi^+\pi^-\mu^+\mu^-) < 1.4 \times 10^{-9},$$
$$\mathcal{B}(K^0_L \to \pi^+\pi^-\mu^+\mu^-) < 6.6 \times 10^{-7},$$

where the limit on each decay mode assumes the absence of the other.

In summary, a search for the $K^0_{S(L)} \to \pi^+\pi^-\mu^+\mu^-$ decays has been performed using pp collision data recorded at LHCb between 2016 and 2018, corresponding to an integrated luminosity of 5.4 fb^{-1}. No evidence for signal is found, and an upper limit for each mode is reported for the first time.

ACKNOWLEDGMENTS

We express our gratitude to our colleagues in the CERN accelerator departments for the excellent performance of the LHC. We thank the technical and administrative staff at the LHCb institutes. We acknowledge support from CERN and from the following national agencies: ARC (Australia); CAPES, CNPq, FAPERJ, and FINEP (Brazil); MOST and NSFC (China); CNRS/IN2P3 and CEA (France); BMFTR, DFG, and MPG (Germany); INFN (Italy); NWO (Netherlands); MNiSW and NCN (Poland); MCID/IFA (Romania); MICIU and AEI (Spain); SNSF and SER (Switzerland); NASU (Ukraine); STFC (United Kingdom); DOE NP and NSF (USA). We acknowledge the computing resources that are provided by ARDC (Australia), CBPF (Brazil), CERN, IHEP, and LZU (China), IN2P3 (France), KIT and DESY (Germany), INFN (Italy), SURF (Netherlands), Polish WLCG (Poland), IFIN-HH (Romania), PIC (Spain), CSCS (Switzerland), and GridPP (United Kingdom). We are indebted to the communities behind the multiple open-source software packages on which we depend. Individual groups or members have received support from RTP (Australia), Key Research Program of Frontier Sciences of CAS, CAS PIFI, CAS CCEPP, Fundamental Research Funds for the Central Universities, and Sci. & Tech. Program of Guangzhou (China); Minciencias (Colombia); EPLANET, Marie Skłodowska-Curie Actions, ERC, and NextGenerationEU (European Union); A*MIDEX, ANR, IPhU, and Labex P2IO, and Région Auvergne-Rhône-Alpes (France); Alexander-von-Humboldt Foundation (Germany); ICSC (Italy); Severo Ochoa and María de Maeztu Units of Excellence, GVA, XuntaGal, GENCAT, InTalent-Inditex, and Prog. Atracción Talento CM (Spain); the Leverhulme Trust, the Royal Society, and UKRI (United Kingdom).

DATA AVAILABILITY

The data that support the findings of this article are openly available on [43].

APPENDIX: ARMENTEROS-PODOLANSKI REQUIREMENT

As described in Sec. V, the $K^0_S \to \pi^+\pi^-$ sample is selected using a requirement in the Armenteros-Podolanski plane. Such cut is defined as

$$\left| \left[\left(\left(\alpha \pm \frac{M_p^2 - M_\pi^2}{M_\Lambda^2} \right) \frac{M_\Lambda p_{K^0_S}}{2p^* \sqrt{p^2_{K^0_S} + M^2_\Lambda}} \right)^2 + \frac{p_{\mathrm{T}}^2}{(p^*)^2} \right] - 1 \right| > 0.3,$$

where, $\alpha = \frac{p_{\mathrm{L}}^+ - p_{\mathrm{L}}^-}{p_{\mathrm{L}}^+ + p_{\mathrm{L}}^-}$ is the longitudinal momentum asymmetry between the positive and negative final-state tracks, p_{L} and p_{T} are the longitudinal and transverse track momentum with respect to the origin particle momentum in the laboratory frame, and $p^* \equiv [(M^2_\Lambda - M^2_p - M^2_\pi)^2 - 4M^2_p M^2_\pi]/(4M^2_\Lambda)$ is the magnitude of final-state track momentum in the center-of-mass frame, assuming a Λ decay.

[1] L. Cappiello, O. Catà, and G. D'Ambrosio, Closing in on the radiative weak chiral couplings, Eur. Phys. J. C **78**, 265 (2018).

[2] L. M. Sehgal and M. Wanninger, *CP* violation in the decay $K^0_L \to \pi^+\pi^-e^+e^-$, Phys. Rev. D **46**, 1035 (1992); **46**, 5209(E) (1992).

[3] J. Adams *et al.* (KTeV Collaboration), Measurement of the branching fraction of the decay $K_L \to \pi^+\pi^-e^+e^-$, Phys. Rev. Lett. **80**, 4123 (1998).

[4] Y. Takeuchi *et al.*, Observation of the decay mode $K_{(L)} \to \pi^+\pi^-e^+e^-$, Phys. Lett. B **443**, 409 (1998).

[5] NA48 Collaboration, Investigation of $K^0_{L,S} \to \pi^+\pi^-e^+e^-$ decays, Eur. Phys. J. C **30**, 33 (2003).

[6] J. R. Batley *et al.* (NA48/1 Collaboration), Precision measurement of the ratio $\mathrm{BR}(K_S \to \pi^+\pi^-e^+e^-)/\mathrm{BR}(K_L \to \pi^+\pi^-\pi^0_D)$, Phys. Lett. B **694**, 301 (2011).

[7] P. Heiliger and L. M. Sehgal, Direct and indirect *CP* violation in the decay $K_L \to \pi^+\pi^-e^+e^-$, Phys. Rev. D **48**, 4146 (1993); **60**, 079902(E) (1999).

[8] H. Pichl, $K \to \pi\pi e^+e^-$ decays and chiral low-energy constants, Eur. Phys. J. C **20**, 371 (2001).

[9] A. A. Alves, Jr. *et al.*, Prospects for measurements with strange hadrons at LHCb, J. High Energy Phys. 05 (2019) 048.

[10] R. Aaij *et al.* (LHCb Collaboration), Constraints on the $K^0_S \to \mu^+\mu^-$ branching fraction, Phys. Rev. Lett. **125**, 1231801 (2020).

[11] R. Aaij *et al.* (LHCb Collaboration), Search for $K^0_{S(L)} \to \mu^+\mu^-\mu^+\mu^-$ decays at LHCb, Phys. Rev. D **108**, L031102 (2023).

[12] S. Navas *et al.* (Particle Data Group), Review of particle physics, Phys. Rev. D **110**, 030001 (2024).

[13] G. D'Ambrosio, A. Dery, Y. Grossman, T. Kitahara, R. Marchevski, D. M. Santos, and S. Schacht, *CP* violation in $K \to \mu^+\mu^-$ with and without time dependence through a tagged analysis, J. High Energy Phys. 09 (2025) 190.

[14] A. A. Alves, Jr. *et al.* (LHCb Collaboration), The LHCb detector at the LHC, J. Instrum. **3**, S08005 (2008).

[15] R. Aaij *et al.* (LHCb Collaboration), LHCb detector performance, Int. J. Mod. Phys. A **30**, 1530022 (2015).

[16] R. Aaij *et al.*, Performance of the LHCb vertex locator, J. Instrum. **9**, P09007 (2014).

[17] P. d'Argent *et al.*, Improved performance of the LHCb outer tracker in LHC Run 2, J. Instrum. **12**, P11016 (2017).

[18] M. Adinolfi *et al.*, Performance of the LHCb RICH detector at the LHC, Eur. Phys. J. C **73**, 2431 (2013).

[19] A. A. Alves, Jr. *et al.*, Performance of the LHCb muon system, J. Instrum. **8**, P02022 (2013).

[20] R. Aaij *et al.*, The LHCb trigger and its performance in 2011, J. Instrum. **8**, P04022 (2013).

[21] R. Aaij *et al.*, Optimization of the muon reconstruction algorithms for LHCb Run 2, Report No. LHCb-PUB-2017-007, CERN, 2017.

[22] F. Dettori, D. Martinez Santos, and J. Prisciandaro, Low-p_T dimuon triggers at LHCb in Run 2, Report No. LHCb-PUB-2017-023, CERN, 2017.

[23] N. Grieser *et al.*, The LHCb stripping project: Sustainable legacy data processing for high-energy physics, Comput. Software Big Sci. **9**, 21 (2025).

[24] T. Sjöstrand, S. Mrenna, and P. Skands, A brief introduction to PYTHIA 8.1, Comput. Phys. Commun. **178**, 852 (2008).

[25] T. Sjöstrand, S. Mrenna, and P. Skands, PYTHIA 6.4 physics and manual, J. High Energy Phys. 05 (2006) 026.

[26] I. Belyaev *et al.*, Handling of the generation of primary events in Gauss, the LHCb simulation framework, J. Phys. Conf. Ser. **331**, 032047 (2011).

[27] D. J. Lange, The EvtGen particle decay simulation package, Nucl. Instrum. Methods Phys. Res., Sect. A **462**, 152 (2001).

[28] N. Davidson, T. Przedzinski, and Z. Was, PHOTOS interface in C++: Technical and physics documentation, Comput. Phys. Commun. **199**, 86 (2016).

[29] J. Allison *et al.* (Geant4 Collaboration), Geant4 developments and applications, IEEE Trans. Nucl. Sci. **53**, 270 (2006).

[30] S. Agostinelli *et al.* (Geant4 Collaboration), Geant4: A simulation toolkit, Nucl. Instrum. Methods Phys. Res., Sect. A **506**, 250 (2003).

[31] M. Clemencic, G. Corti, S. Easo, C. R. Jones, S. Miglioranzi, M. Pappagallo, and P. Robbe, The LHCb simulation application, Gauss: Design, evolution and experience, J. Phys. Conf. Ser. **331**, 032023 (2011).

[32] L. Breiman, J. H. Friedman, R. A. Olshen, and C. J. Stone, *Classification and Regression Trees* (Wadsworth International Group, Belmont, CA, 1984).

[33] Y. Freund and R. E. Schapire, A decision-theoretic generalization of on-line learning and an application to boosting, J. Comput. Syst. Sci. **55**, 119 (1997).

[34] T. Chen and C. Guestrin, XGBoost: A scalable tree boosting system, in *Proceedings of the 22nd ACM SIGKDD International Conference on Knowledge Discovery and Data Mining, KDD '16* (ACM, New York, NY, 2016), pp. 785–794.

[35] M. Alexander *et al.*, Mapping the material in the LHCb vertex locator using secondary hadronic interactions, J. Instrum. **13**, P06008 (2018).

[36] F. Pedregosa *et al.*, scikit-learn/scikit-learn: v1.4.0, Zenodo (2024), 10.5281/zenodo.10666857.

[37] T. Skwarnicki, A study of the radiative cascade transitions between the Upsilon-prime and Upsilon resonances, Ph.D. thesis, Institute of Nuclear Physics, Krakow, 1986, DESY-F31-86-02.

[38] J. Podolanski and R. Armenteros, III. Analysis of V-events, Phil. Mag. **45**, 13 (1954).

[39] LHCb Collaboration, Measurement of the track reconstruction efficiency at LHCb, J. Instrum. **10**, P02007 (2015).

[40] F. Ambrosino *et al.* (KLOE Collaboration), Measurement of the K_L meson lifetime with the KLOE detector, Phys. Lett. B **626**, 15 (2005).

[41] F. Ambrosino *et al.* (KLOE Collaboration), Measurements of the absolute branching ratios for the dominant K_L decays, the K_L lifetime, and V_{us} with the KLOE detector, Phys. Lett. B **632**, 43 (2006).

[42] D. Babusci *et al.* (KLOE-2 Collaboration), Measurement of the branching fraction for the decay $K_S \to \pi\mu\nu$ with the KLOE detector, Phys. Lett. B **804**, 135378 (2020).

[43] https://cds.cern.ch/record/2948383.

R. Aaij,[38] A. S. W. Abdelmotteleb,[58] C. Abellan Beteta,[52] F. Abudinén,[58] T. Ackernley,[62] A. A. Adefisoye,[70] B. Adeva,[48] M. Adinolfi,[56] P. Adlarson,[86] C. Agapopoulou,[14] C. A. Aidala,[88] Z. Ajaltouni,[11] S. Akar,[11] K. Akiba,[38] P. Albicocco,[28] J. Albrecht,[19,a] R. Aleksiejunas,[82] F. Alessio,[50] P. Alvarez Cartelle,[57] R. Amalric,[16] S. Amato,[3] J. L. Amey,[56] Y. Amhis,[14] L. An,[6] L. Anderlini,[27] M. Andersson,[52] P. Andreola,[52] M. Andreotti,[26] S. Andres Estrada,[45] A. Anelli,[31,50,b] D. Ao,[7] C. Arata,[12] F. Archilli,[37,c] Z. Areg,[70] M. Argenton,[26] S. Arguedas Cuendis,[9,50] L. Arnone,[31,b] A. Artamonov,[44] M. Artuso,[70] E. Aslanides,[13] R. Ataíde Da Silva,[51] M. Atzeni,[66] B. Audurier,[12] J. A. Authier,[15] D. Bacher,[65] I. Bachiller Perea,[51] S. Bachmann,[22] M. Bachmayer,[51] J. J. Back,[58] P. Baladron Rodriguez,[48] V. Balagura,[15] A. Balboni,[26] W. Baldini,[26] Z. Baldwin,[80] L. Balzani,[19] H. Bao,[7] J. Baptista de Souza Leite,[2] C. Barbero Pretel,[48,12] M. Barbetti,[27] I. R. Barbosa,[71] R. J. Barlow,[64] M. Barnyakov,[25] S. Barsuk,[14] W. Barter,[60] J. Bartz,[70] S. Bashir,[40] B. Batsukh,[5] P. B. Battista,[14] A. Bay,[51] A. Beck,[66] M. Becker,[19] F. Bedeschi,[35] I. B. Bediaga,[2] N. A. Behling,[19] S. Belin,[48] A. Bellavista,[25] K. Belous,[44] I. Belov,[29] I. Belyaev,[36] G. Benane,[13] G. Bencivenni,[28] E. Ben-Haim,[16] A. Berezhnoy,[44] R. Bernet,[52] S. Bernet Andres,[47] A. Bertolin,[33] F. Betti,[60] J. Bex,[57] O. Bezshyyko,[87] S. Bhattacharya,[81] J. Bhom,[41] M. S. Bieker,[18] N. V. Biesuz,[26] A. Biolchini,[38] M. Birch,[63] F. C. R. Bishop,[10] A. Bitadze,[64] A. Bizzeti,[27,d] T. Blake,[58,e] F. Blanc,[51] J. E. Blank,[19] S. Blusk,[70] V. Bocharnikov,[44] J. A. Boelhauve,[19] O. Boente Garcia,[50] T. Boettcher,[69] A. Bohare,[60] A. Boldyrev,[44] C. S. Bolognani,[84] R. Bolzonella,[26,f] R. B. Bonacci,[1] N. Bondar,[44,50] A. Bordelius,[50] F. Borgato,[33,50] S. Borghi,[64] M. Borsato,[31,b] J. T. Borsuk,[85] E. Bottalico,[62] S. A. Bouchiba,[51] M. Bovill,[65] T. J. V. Bowcock,[62] A. Boyer,[50] C. Bozzi,[26] J. D. Brandenburg,[89] A. Brea Rodriguez,[51] N. Breer,[19] J. Brodzicka,[41] J. Brown,[62] D. Brundu,[32] E. Buchanan,[60] M. Burgos Marcos,[84] A. T. Burke,[64] C. Burr,[50] C. Buti,[27] J. S. Butter,[57] J. Buytaert,[50] W. Byczynski,[50] S. Cadeddu,[32] H. Cai,[76] Y. Cai,[5] A. Caillet,[16] R. Calabrese,[26,f] S. Calderon Ramirez,[9] L. Calefice,[46] M. Calvi,[31,b] M. Calvo Gomez,[47] P. Camargo Magalhaes,[2,g] J. I. Cambon Bouzas,[48] P. Campana,[28] A. F. Campoverde Quezada,[7] S. Capelli,[31] M. Caporale,[25] L. Capriotti,[26] R. Caravaca-Mora,[9] A. Carbone,[25,h] L. Carcedo Salgado,[48] R. Cardinale,[29,i] A. Cardini,[32] P. Carniti,[31] L. Carus,[22] A. Casais Vidal,[66] R. Caspary,[22] G. Casse,[62] M. Cattaneo,[50] G. Cavallero,[26] V. Cavallini,[26,f] S. Celani,[50] I. Celestino,[35,j] S. Cesare,[30,k] A. J. Chadwick,[62] I. Chahrour,[88] H. Chang,[4,l] M. Charles,[16] Ph. Charpentier,[50] E. Chatzianagnostou,[38] R. Cheaib,[81] M. Chefdeville,[10] C. Chen,[57] J. Chen,[51] S. Chen,[5] Z. Chen,[7] A. Chen Hu,[63] M. Cherif,[12] A. Chernov,[41] S. Chernyshenko,[54] X. Chiotopoulos,[84] V. Chobanova,[45] M. Chrzaszcz,[41] A. Chubykin,[44] V. Chulikov,[28,36,50] P. Ciambrone,[28] X. Cid Vidal,[48] G. Ciezarek,[50] P. Cifra,[38] P. E. L. Clarke,[60] M. Clemencic,[50] H. V. Cliff,[57] J. Closier,[50] C. Cocha Toapaxi,[22] V. Coco,[50] J. Cogan,[13] E. Cogneras,[11] L. Cojocariu,[43] S. Collaviti,[51] P. Collins,[50] T. Colombo,[50] M. Colonna,[19] A. Comerma-Montells,[46] L. Congedo,[24] J. Connaughton,[58] A. Contu,[32] N. Cooke,[61] G. Cordova,[35,j] C. Coronel,[67] I. Corredoira,[12] A. Correia,[16] G. Corti,[50] J. Cottee Meldrum,[56] B. Couturier,[50] D. C. Craik,[52] M. Cruz Torres,[2,m] E. Curras Rivera,[51] R. Currie,[60] C. L. Da Silva,[69] S. Dadabaev,[44] X. Dai,[4] E. Dall'Occo,[50] J. Dalseno,[45] C. D'Ambrosio,[63] J. Daniel,[11] G. Darze,[3] A. Davidson,[58] J. E. Davies,[64] O. De Aguiar Francisco,[64] C. De Angelis,[32,n] F. De Benedetti,[50] J. de Boer,[38] K. De Bruyn,[83] S. De Capua,[64] M. De Cian,[64,50] U. De Freitas Carneiro Da Graca,[2,o] E. De Lucia,[28] J. M. De Miranda,[2] L. De Paula,[3] M. De Serio,[24,p] P. De Simone,[28] F. De Vellis,[19] J. A. de Vries,[84] F. Debernardis,[24] D. Decamp,[10] S. Dekkers,[1] L. Del Buono,[16] B. Delaney,[66] H.-P. Dembinski,[19] J. Deng,[8] V. Denysenko,[52] O. Deschamps,[11] F. Dettori,[32,n] B. Dey,[81] P. Di Nezza,[28] I. Diachkov,[44] S. Didenko,[44] S. Ding,[70] Y. Ding,[51] L. Dittmann,[22] V. Dobishuk,[54] A. D. Docheva,[61] A. Doheny,[58] C. Dong,[4,l] A. M. Donohoe,[23] F. Dordei,[32] A. C. dos Reis,[2] A. D. Dowling,[70] L. Dreyfus,[13] W. Duan,[74] P. Duda,[85] L. Dufour,[50] V. Duk,[34] P. Durante,[50] M. M. Duras,[85] J. M. Durham,[69] O. D. Durmus,[81] A. Dziurda,[41] A. Dzyuba,[44] S. Easo,[59] E. Eckstein,[18] U. Egede,[1] A. Egorychev,[44] V. Egorychev,[44] S. Eisenhardt,[60] E. Ejopu,[62] L. Eklund,[86] M. Elashri,[67] D. Elizondo Blanco,[9] J. Ellbracht,[19] S. Ely,[63] A. Ene,[43] J. Eschle,[70] S. Esen,[22] T. Evans,[38] F. Fabiano,[32] S. Faghih,[67] L. N. Falcao,[31,b] B. Fang,[7] R. Fantechi,[35] L. Fantini,[34,q] M. Faria,[51] K. Farmer,[60] F. Fassin,[83,38] D. Fazzini,[31,b] L. Felkowski,[85] M. Feng,[5,7] A. Fernandez Casani,[49] M. Fernandez Gomez,[48] A. D. Fernez,[68] F. Ferrari,[25,h] F. Ferreira Rodrigues,[3] M. Ferrillo,[52] M. Ferro-Luzzi,[50] S. Filippov,[44] R. A. Fini,[24] M. Fiorini,[26,f] M. Firlej,[40] K. L. Fischer,[65] D. S. Fitzgerald,[88] C. Fitzpatrick,[64] T. Fiutowski,[40] F. Fleuret,[15] A. Fomin,[53] M. Fontana,[25] L. A. Foreman,[64] R. Forty,[50] D. Foulds-Holt,[60]

V. Franco Lima,[3] M. Franco Sevilla,[68] M. Frank,[50] E. Franzoso,[26,f] G. Frau,[64] C. Frei,[50] D. A. Friday,[64,50] J. Fu,[7] Q. Führing,[19,57,a] T. Fulghesu,[13] G. Galati,[24] M. D. Galati,[38] A. Gallas Torreira,[48] D. Galli,[25,h] S. Gambetta,[60] M. Gandelman,[3] P. Gandini,[30] B. Ganie,[64] H. Gao,[7] R. Gao,[65] T. Q. Gao,[57] Y. Gao,[8] Y. Gao,[6] Y. Gao,[8] L. M. Garcia Martin,[51] P. Garcia Moreno,[46] J. García Pardiñas,[66] P. Gardner,[68] L. Garrido,[46] C. Gaspar,[50] A. Gavrikov,[33] L. L. Gerken,[19] E. Gersabeck,[20] M. Gersabeck,[20] T. Gershon,[58] S. Ghizzo,[29,i] Z. Ghorbanimoghaddam,[56] F. I. Giasemis,[16,r] V. Gibson,[57] H. K. Giemza,[42] A. L. Gilman,[67] M. Giovannetti,[28] A. Gioventù,[46] L. Girardey,[64,59] M. A. Giza,[41] F. C. Glaser,[14,22] V. V. Gligorov,[16] C. Göbel,[71] L. Golinka-Bezshyyko,[87] E. Golobardes,[47] D. Golubkov,[44] A. Golutvin,[63,50] S. Gomez Fernandez,[46] W. Gomulka,[40] I. Gonçales Vaz,[50] F. Goncalves Abrantes,[65] M. Goncerz,[41] G. Gong,[4,l] J. A. Gooding,[19] I. V. Gorelov,[44] C. Gotti,[31] E. Govorkova,[66] J. P. Grabowski,[30] L. A. Granado Cardoso,[50] E. Graugés,[46] E. Graverini,[51,s] L. Grazette,[58] G. Graziani,[27] A. T. Grecu,[43] N. A. Grieser,[67] L. Grillo,[61] S. Gromov,[44] C. Gu,[15] M. Guarise,[26] L. Guerry,[11] A.-K. Guseinov,[51] E. Gushchin,[44] Y. Guz,[6,50] T. Gys,[50] K. Habermann,[18] T. Hadavizadeh,[1] C. Hadjivasiliou,[68] G. Haefeli,[51] C. Haen,[50] S. Haken,[57] G. Hallett,[58] P. M. Hamilton,[68] J. Hammerich,[62] Q. Han,[33] X. Han,[22,50] S. Hansmann-Menzemer,[22] L. Hao,[7] N. Harnew,[65] T. H. Harris,[1] M. Hartmann,[14] S. Hashmi,[40] J. He,[7,t] N. Heatley,[14] A. Hedes,[64] F. Hemmer,[50] C. Henderson,[67] R. Henderson,[14] R. D. L. Henderson,[1] A. M. Hennequin,[50] K. Hennessy,[62] L. Henry,[51] J. Herd,[63] P. Herrero Gascon,[22] J. Heuel,[17] A. Heyn,[13] A. Hicheur,[3] G. Hijano Mendizabal,[52] J. Horswill,[64] R. Hou,[8] Y. Hou,[11] D. C. Houston,[61] N. Howarth,[62] W. Hu,[7] X. Hu,[4] W. Hulsbergen,[38] R. J. Hunter,[58] M. Hushchyn,[44] D. Hutchcroft,[62] M. Idzik,[40] D. Ilin,[44] P. Ilten,[67] A. Iniukhin,[44] A. Iohner,[10] A. Ishteev,[44] K. Ivshin,[44] H. Jage,[17] S. J. Jaimes Elles,[78,49,50] S. Jakobsen,[50] T. Jakoubek,[79] E. Jans,[38] B. K. Jashal,[49] A. Jawahery,[68] C. Jayaweera,[55] V. Jevtic,[19] Z. Jia,[16] E. Jiang,[68] X. Jiang,[5,7] Y. Jiang,[7] Y. J. Jiang,[6] E. Jimenez Moya,[9] N. Jindal,[89] M. John,[65] A. John Rubesh Rajan,[23] D. Johnson,[55] C. R. Jones,[57] S. Joshi,[42] B. Jost,[50] J. Juan Castella,[57] N. Jurik,[50] I. Juszczak,[41] K. Kalecinska,[40] D. Kaminaris,[51] S. Kandybei,[53] M. Kane,[60] Y. Kang,[4,l] C. Kar,[11] M. Karacson,[50] A. Kauniskangas,[51] J. W. Kautz,[67] M. K. Kazanecki,[41] F. Keizer,[50] M. Kenzie,[57] T. Ketel,[38] B. Khanji,[70] A. Kharisova,[44] S. Kholodenko,[63,50] G. Khreich,[14] T. Kirn,[17] V. S. Kirsebom,[31,b] S. Klaver,[39] N. Kleijne,[35,j] A. Kleimenova,[51] D. K. Klekots,[87] K. Klimaszewski,[42] M. R. Kmiec,[42] T. Knospe,[19] R. Kolb,[22] S. Koliiev,[54] L. Kolk,[19] A. Konoplyannikov,[6] P. Kopciewicz,[50] P. Koppenburg,[38] A. Korchin,[53] M. Korolev,[44] I. Kostiuk,[38] O. Kot,[54] S. Kotriakhova, E. Kowalczyk,[68] A. Kozachuk,[44] P. Kravchenko,[44] L. Kravchuk,[44] O. Kravcov,[82] M. Kreps,[58] P. Krokovny,[44] W. Krupa,[70] W. Krzemien,[42] O. Kshyvanskyi,[54] S. Kubis,[85] M. Kucharczyk,[41] V. Kudryavtsev,[44] E. Kulikova,[44] A. Kupsc,[86] V. Kushnir,[53] B. Kutsenko,[13] J. Kvapil,[69] I. Kyryllin,[53] D. Lacarrere,[50] P. Laguarta Gonzalez,[46] A. Lai,[32] A. Lampis,[32] D. Lancierini,[63] C. Landesa Gomez,[48] J. J. Lane,[1] G. Lanfranchi,[28] C. Langenbruch,[22] J. Langer,[19] T. Latham,[58] F. Lazzari,[35,50,s] C. Lazzeroni,[55] R. Le Gac,[13] H. Lee,[62] R. Lefèvre,[11] A. Leflat,[44] S. Legotin,[44] M. Lehuraux,[58] E. Lemos Cid,[50] O. Leroy,[13] T. Lesiak,[41] E. D. Lesser,[50] B. Leverington,[22] A. Li,[4,l] C. Li,[4,l] C. Li,[13] H. Li,[74] J. Li,[8] K. Li,[77] L. Li,[64] M. Li,[8] P. Li,[7] P.-R. Li,[75] Q. Li,[5,7] T. Li,[73] T. Li,[74] Y. Li,[8] Y. Li,[5] Y. Li,[4] Z. Lian,[4,l] Q. Liang,[8] X. Liang,[70] Z. Liang,[32] S. Libralon,[49] A. L. Lightbody,[12] C. Lin,[7] T. Lin,[59] R. Lindner,[50] H. Linton,[63] R. Litvinov,[32] D. Liu,[8] F. L. Liu,[1] G. Liu,[74] K. Liu,[75] S. Liu,[5] W. Liu,[8] Y. Liu,[60] Y. Liu,[75] Y. L. Liu,[63] G. Loachamin Ordonez,[71] I. Lobo,[1] A. Lobo Salvia,[46] A. Loi,[32] T. Long,[57] F. C. L. Lopes,[2,g] J. H. Lopes,[3] A. Lopez Huertas,[46] C. Lopez Iribarnegaray,[48] S. López Soliño,[48] Q. Lu,[15] C. Lucarelli,[50] D. Lucchesi,[33,u] M. Lucio Martinez,[49] Y. Luo,[6] A. Lupato,[33,v] E. Luppi,[26,f] K. Lynch,[23] X.-R. Lyu,[7] G. M. Ma,[4,l] H. Ma,[73] S. Maccolini,[19] F. Machefert,[14] F. Maciuc,[43] B. Mack,[70] I. Mackay,[65] L. M. Mackey,[70] L. R. Madhan Mohan,[57] M. J. Madurai,[55] D. Magdalinski,[38] D. Maisuzenko,[44] J. J. Malczewski,[41] S. Malde,[65] L. Malentacca,[50] A. Malinin,[44] T. Maltsev,[44] G. Manca,[32,n] G. Mancinelli,[13] C. Mancuso,[14] R. Manera Escalero,[46] F. M. Manganella,[37] D. Manuzzi,[25] D. Marangotto,[30,k] J. F. Marchand,[10] R. Marchevski,[51] U. Marconi,[25] E. Mariani,[16] S. Mariani,[50] C. Marin Benito,[46] J. Marks,[22] A. M. Marshall,[56] L. Martel,[65] G. Martelli,[34] G. Martellotti,[36] L. Martinazzoli,[50] M. Martinelli,[31,b] D. Martinez Gomez,[83] D. Martinez Santos,[45] F. Martinez Vidal,[49] A. Martorell Granollers I,[47] A. Massafferri,[2] R. Matev,[50] A. Mathad,[50] V. Matiunin,[44] C. Matteuzzi,[70] K. R. Mattioli,[15] A. Mauri,[63] E. Maurice,[15] J. Mauricio,[46] P. Mayencourt,[51] J. Mazorra de Cos,[49] M. Mazurek,[42] M. McCann,[63] N. T. McHugh,[61] A. McNab,[64] R. McNulty,[23]

B. Meadows,[67] G. Meier,[19] D. Melnychuk,[42] D. Mendoza Granada,[16] P. Menendez Valdes Perez,[48] F. M. Meng,[4,l] M. Merk,[38,84] A. Merli,[51,30] L. Meyer Garcia,[68] D. Miao,[5,7] H. Miao,[7] M. Mikhasenko,[80] D. A. Milanes,[78,w] A. Minotti,[31,b] E. Minucci,[28] T. Miralles,[11] B. Mitreska,[64] D. S. Mitzel,[19] R. Mocanu,[43] A. Modak,[59] L. Moeser,[19] R. D. Moise,[17] E. F. Molina Cardenas,[88] T. Mombächer,[67] M. Monk,[57] T. Monnard,[51] S. Monteil,[11] A. Morcillo Gomez,[48] G. Morello,[28] M. J. Morello,[35,j] M. P. Morgenthaler,[22] A. Moro,[31,b] J. Moron,[40] W. Morren,[38] A. B. Morris,[50] A. G. Morris,[13] R. Mountain,[70] Z. M. Mu,[6] E. Muhammad,[58] F. Muheim,[60] M. Mulder,[83] K. Müller,[52] F. Muñoz-Rojas,[9] R. Murta,[63] V. Mytrochenko,[53] P. Naik,[62] T. Nakada,[51] R. Nandakumar,[59] T. Nanut,[50] G. Napoletano,[51] I. Nasteva,[3] M. Needham,[60] E. Nekrasova,[44] N. Neri,[30,k] S. Neubert,[18] N. Neufeld,[50] P. Neustroev,[44] J. Nicolini,[50] D. Nicotra,[84] E. M. Niel,[15] N. Nikitin,[44] L. Nisi,[19] Q. Niu,[75] P. Nogarolli,[3] P. Nogga,[18] C. Normand,[56] J. Novoa Fernandez,[48] G. Nowak,[67] C. Nunez,[88] H. N. Nur,[61] A. Oblakowska-Mucha,[40] V. Obraztsov,[44] T. Oeser,[17] A. Okhotnikov,[44] O. Okhrimenko,[54] R. Oldeman,[32,n] F. Oliva,[60,50] E. Olivart Pino,[46] M. Olocco,[19] R. H. O'Neil,[50] J. S. Ordonez Soto,[11] D. Osthues,[19] J. M. Otalora Goicochea,[3] P. Owen,[52] A. Oyanguren,[49] O. Ozcelik,[50] F. Paciolla,[35,x] A. Padee,[42] K. O. Padeken,[18] B. Pagare,[48] T. Pajero,[50] A. Palano,[24] L. Palini,[30] M. Palutan,[28] C. Pan,[76] X. Pan,[4,l] S. Panebianco,[12] S. Paniskaki,[50,33] G. Panshin,[5] L. Paolucci,[64] A. Papanestis,[59] M. Pappagallo,[24,p] L. L. Pappalardo,[26] C. Pappenheimer,[67] C. Parkes,[64] D. Parmar,[80] G. Passaleva,[27] D. Passaro,[35,50,j] A. Pastore,[24] M. Patel,[63] J. Patoc,[65] C. Patrignani,[25,h] A. Paul,[70] C. J. Pawley,[84] A. Pellegrino,[38] J. Peng,[5,7] X. Peng,[75] M. Pepe Altarelli,[28] S. Perazzini,[25] D. Pereima,[44] H. Pereira Da Costa,[69] M. Pereira Martinez,[48] A. Pereiro Castro,[48] C. Perez,[47] P. Perret,[11] A. Perrevoort,[83] A. Perro,[50,13] M. J. Peters,[67] K. Petridis,[56] A. Petrolini,[29,i] S. Pezzulo,[29,i] J. P. Pfaller,[67] H. Pham,[70] L. Pica,[35,j] M. Piccini,[34] L. Piccolo,[32] B. Pietrzyk,[10] G. Pietrzyk,[14] R. N. Pilato,[62] D. Pinci,[36] F. Pisani,[50] M. Pizzichemi,[31,50,b] V. M. Placinta,[43] M. Plo Casasus,[48] T. Poeschl,[50] F. Polci,[16] M. Poli Lener,[28] A. Poluektov,[13] N. Polukhina,[44] I. Polyakov,[64] E. Polycarpo,[3] S. Ponce,[50] D. Popov,[7,50] K. Popp,[19] S. Poslavskii,[44] K. Prasanth,[60] C. Prouve,[45] D. Provenzano,[32,50,n] V. Pugatch,[54] A. Puicercus Gomez,[50] G. Punzi,[35,s] J. R. Pybus,[69] Q. Q. Qian,[6] W. Qian,[7] N. Qin,[4,l] R. Quagliani,[50] R. I. Rabadan Trejo,[58] R. Racz,[82] J. H. Rademacker,[56] M. Rama,[35] M. Ramírez García,[88] V. Ramos De Oliveira,[71] M. Ramos Pernas,[58] M. S. Rangel,[3] F. Ratnikov,[44] G. Raven,[39] M. Rebollo De Miguel,[49] F. Redi,[30,v] J. Reich,[56] F. Reiss,[20] Z. Ren,[7] P. K. Resmi,[65] M. Ribalda Galvez,[46] R. Ribatti,[51] G. Ricart,[15,12] D. Riccardi,[35,j] S. Ricciardi,[59] K. Richardson,[66] M. Richardson-Slipper,[57] F. Riehn,[19] K. Rinnert,[62] P. Robbe,[14,50] G. Robertson,[61] E. Rodrigues,[62] A. Rodriguez Alvarez,[46] E. Rodriguez Fernandez,[48] J. A. Rodriguez Lopez,[78] E. Rodriguez Rodriguez,[50] J. Roensch,[19] A. Rogachev,[44] A. Rogovskiy,[59] D. L. Rolf,[19] P. Roloff,[50] V. Romanovskiy,[67] A. Romero Vidal,[48] G. Romolini,[26,50] F. Ronchetti,[51] T. Rong,[6] M. Rotondo,[28] S. R. Roy,[22] M. S. Rudolph,[70] M. Ruiz Diaz,[22] R. A. Ruiz Fernandez,[48] J. Ruiz Vidal,[84] J. J. Saavedra-Arias,[9] J. J. Saborido Silva,[48] S. E. R. Sacha Emile R.,[50] N. Sagidova,[44] D. Sahoo,[81] N. Sahoo,[55] B. Saitta,[32] M. Salomoni,[31,50,b] I. Sanderswood,[49] R. Santacesaria,[36] C. Santamarina Rios,[48] M. Santimaria,[28] L. Santoro,[2] E. Santovetti,[37] A. Saputi,[26,50] D. Saranin,[44] A. Sarnatskiy,[83] G. Sarpis,[50] M. Sarpis,[82] C. Satriano,[36] A. Satta,[37] M. Saur,[75] D. Savrina,[44] H. Sazak,[17] F. Sborzacchi,[50,28] A. Scarabotto,[19] S. Schael,[17] S. Scherl,[62] M. Schiller,[22] H. Schindler,[50] M. Schmelling,[21] B. Schmidt,[50] N. Schmidt,[69] S. Schmitt,[66] H. Schmitz,[18] O. Schneider,[51] A. Schopper,[63] N. Schulte,[19] M. H. Schune,[14] G. Schwering,[17] B. Sciascia,[28] A. Sciuccati,[50] G. Scriven,[84] I. Segal,[80] S. Sellam,[48] A. Semennikov,[44] T. Senger,[52] M. Senghi Soares,[39] A. Sergi,[29,i] N. Serra,[52] L. Sestini,[27] A. Seuthe,[19] B. Sevilla Sanjuan,[47] Y. Shang,[6] D. M. Shangase,[88] M. Shapkin,[44] R. S. Sharma,[70] I. Shchemerov,[44] L. Shchutska,[51] T. Shears,[62] L. Shekhtman,[44] Z. Shen,[38] S. Sheng,[5,7] V. Shevchenko,[44] B. Shi,[7] Q. Shi,[7] W. S. Shi,[74] Y. Shimizu,[14] E. Shmanin,[25] R. Shorkin,[44] J. D. Shupperd,[70] R. Silva Coutinho,[2] G. Simi,[33,u] S. Simone,[24,p] M. Singha,[81] N. Skidmore,[58] T. Skwarnicki,[70] M. W. Slater,[55] E. Smith,[66] K. Smith,[69] M. Smith,[63] L. Soares Lavra,[60] M. D. Sokoloff,[67] F. J. P. Soler,[61] A. Solomin,[56] A. Solovev,[44] K. Solovieva,[20] N. S. Sommerfeld,[18] R. Song,[1] Y. Song,[51] Y. Song,[4,l] Y. S. Song,[6] F. L. Souza De Almeida,[46] B. Souza De Paula,[3] K. M. Sowa,[40] E. Spadaro Norella,[29,i] E. Spedicato,[25] J. G. Speer,[19] P. Spradlin,[61] F. Stagni,[50] M. Stahl,[80] S. Stahl,[50] S. Stanislaus,[65] M. Stefaniak,[89] E. N. Stein,[50] O. Steinkamp,[52] D. Strekalina,[44] Y. Su,[7] F. Suljik,[65] J. Sun,[32] J. Sun,[64] L. Sun,[76] D. Sundfeld,[2] W. Sutcliffe,[52] P. Svihra,[79] V. Svintozelskyi,[49] K. Swientek,[40] F. Swystun,[57] A. Szabelski,[42] T. Szumlak,[40]

Y. Tan,[4] Y. Tang,[76] Y. T. Tang,[7] M. D. Tat,[22] J. A. Teijeiro Jimenez,[48] A. Terentev,[44] F. Terzuoli,[35,x] F. Teubert,[50] E. Thomas,[50] D. J. D. Thompson,[55] A. R. Thomson-Strong,[60] H. Tilquin,[63] V. Tisserand,[11] S. T'Jampens,[10] M. Tobin,[5,50] T. T. Todorov,[20] L. Tomassetti,[26,f] G. Tonani,[30] X. Tong,[6] T. Tork,[30] D. Torres Machado,[2] L. Toscano,[19] D. Y. Tou,[4,l] C. Trippl,[47] G. Tuci,[22] N. Tuning,[38] L. H. Uecker,[22] A. Ukleja,[40] D. J. Unverzagt,[22] A. Upadhyay,[50] B. Urbach,[60] A. Usachov,[38] A. Ustyuzhanin,[44] U. Uwer,[22] V. Vagnoni,[25,50] A. Vaitkevicius,[82] V. Valcarce Cadenas,[48] G. Valenti,[25] N. Valls Canudas,[50] J. van Eldik,[50] H. Van Hecke,[69] E. van Herwijnen,[63] C. B. Van Hulse,[48,y] R. Van Laak,[51] M. van Veghel,[84] G. Vasquez,[52] R. Vazquez Gomez,[46] P. Vazquez Regueiro,[48] C. Vázquez Sierra,[45] S. Vecchi,[26] J. Velilla Serna,[49] J. J. Velthuis,[56] M. Veltri,[27,z] A. Venkateswaran,[51] M. Verdoglia,[32] M. Vesterinen,[58] W. Vetens,[70] D. Vico Benet,[65] P. Vidrier Villalba,[46] M. Vieites Diaz,[48] X. Vilasis-Cardona,[47] E. Vilella Figueras,[62] A. Villa,[25] P. Vincent,[16] B. Vivacqua,[3] F. C. Volle,[55] D. vom Bruch,[13] N. Voropaev,[44] K. Vos,[84] C. Vrahas,[60] J. Wagner,[19] J. Walsh,[35] E. J. Walton,[1,58] G. Wan,[6] A. Wang,[7] B. Wang,[5] C. Wang,[22] G. Wang,[8] H. Wang,[75] J. Wang,[7] J. Wang,[5] J. Wang,[4,l] J. Wang,[76] M. Wang,[50] N. W. Wang,[7] R. Wang,[56] X. Wang,[8] X. Wang,[74] X. W. Wang,[63] Y. Wang,[77] Y. Wang,[6] Y. H. Wang,[75] Z. Wang,[14] Z. Wang,[30] J. A. Ward,[58,1] M. Waterlaat,[50] N. K. Watson,[55] D. Websdale,[63] Y. Wei,[6] Z. Weida,[7] J. Wendel,[45] B. D. C. Westhenry,[56] C. White,[57] M. Whitehead,[61] E. Whiter,[55] A. R. Wiederhold,[64] D. Wiedner,[19] M. A. Wiegertjes,[38] C. Wild,[65] G. Wilkinson,[65,50] M. K. Wilkinson,[67] M. Williams,[66] M. J. Williams,[50] M. R. J. Williams,[60] R. Williams,[57] S. Williams,[56] Z. Williams,[56] F. F. Wilson,[59] M. Winn,[12] W. Wislicki,[42] M. Witek,[41] L. Witola,[19] T. Wolf,[22] E. Wood,[57] G. Wormser,[14] S. A. Wotton,[57] H. Wu,[70] J. Wu,[8] X. Wu,[76] Y. Wu,[6,57] Z. Wu,[7] K. Wyllie,[50] S. Xian,[74] Z. Xiang,[5] Y. Xie,[8] T. X. Xing,[30] A. Xu,[35,j] L. Xu,[4,l] M. Xu,[50] Z. Xu,[50] Z. Xu,[7] Z. Xu,[5] S. Yadav,[26] K. Yang,[63] X. Yang,[6] Y. Yang,[7] Y. Yang,[81] Z. Yang,[6] V. Yeroshenko,[14] H. Yeung,[64] H. Yin,[8] X. Yin,[7] C. Y. Yu,[6] J. Yu,[73] X. Yuan,[5] Y Yuan,[5,7] J. A. Zamora Saa,[72] M. Zavertyaev,[21] M. Zdybal,[41] F. Zenesini,[25] C. Zeng,[5,7] M. Zeng,[4,l] C. Zhang,[6] D. Zhang,[8] J. Zhang,[7] L. Zhang,[4,l] R. Zhang,[8] S. Zhang,[65] S. L. Zhang,[73] Y. Zhang,[6] Y. Z. Zhang,[4,l] Z. Zhang,[4,l] Y. Zhao,[22] A. Zhelezov,[22] S. Z. Zheng,[6] X. Z. Zheng,[4,l] Y. Zheng,[7] T. Zhou,[6] X. Zhou,[8] Y. Zhou,[7] V. Zhovkovska,[58] L. Z. Zhu,[7] X. Zhu,[4,l] X. Zhu,[8] Y. Zhu,[17] V. Zhukov,[17] J. Zhuo,[49] Q. Zou,[5,7] D. Zuliani,[33,u] and G. Zunica[28]

(LHCb Collaboration)

[1]*School of Physics and Astronomy, Monash University, Melbourne, Australia*
[2]*Centro Brasileiro de Pesquisas Físicas (CBPF), Rio de Janeiro, Brazil*
[3]*Universidade Federal do Rio de Janeiro (UFRJ), Rio de Janeiro, Brazil*
[4]*Department of Engineering Physics, Tsinghua University, Beijing, China*
[5]*Institute of High Energy Physics (IHEP), Beijing, China*
[6]*School of Physics State Key Laboratory of Nuclear Physics and Technology, Peking University, Beijing, China*
[7]*University of Chinese Academy of Sciences, Beijing, China*
[8]*Institute of Particle Physics, Central China Normal University, Wuhan, Hubei, China*
[9]*Consejo Nacional de Rectores (CONARE), San Jose, Costa Rica*
[10]*Université Savoie Mont Blanc, CNRS, IN2P3-LAPP, Annecy, France*
[11]*Université Clermont Auvergne, CNRS/IN2P3, LPC, Clermont-Ferrand, France*
[12]*Université Paris-Saclay, Centre d'Etudes de Saclay (CEA), IRFU, Saclay, France, Gif-Sur-Yvette, France*
[13]*Aix Marseille University, CNRS/IN2P3, CPPM, Marseille, France*
[14]*Université Paris-Saclay, CNRS/IN2P3, IJCLab, Orsay, France*
[15]*Laboratoire Leprince-Ringuet, CNRS/IN2P3, Ecole Polytechnique, Institut Polytechnique de Paris, Palaiseau, France*
[16]*Laboratoire de Physique Nucléaire et de Hautes Énergies (LPNHE), Sorbonne Université, CNRS/IN2P3, F-75005 Paris, France, Paris, France*
[17]*I. Physikalisches Institut, RWTH Aachen University, Aachen, Germany*
[18]*Universität Bonn—Helmholtz-Institut für Strahlen und Kernphysik, Bonn, Germany*
[19]*Fakultät Physik, Technische Universität Dortmund, Dortmund, Germany*
[20]*Physikalisches Institut, Albert-Ludwigs-Universität Freiburg, Freiburg, Germany*
[21]*Max-Planck-Institut für Kernphysik (MPIK), Heidelberg, Germany*

[22]*Physikalisches Institut, Ruprecht-Karls-Universität Heidelberg, Heidelberg, Germany*
[23]*School of Physics, University College Dublin, Dublin, Ireland*
[24]*INFN Sezione di Bari, Bari, Italy*
[25]*INFN Sezione di Bologna, Bologna, Italy*
[26]*INFN Sezione di Ferrara, Ferrara, Italy*
[27]*INFN Sezione di Firenze, Firenze, Italy*
[28]*INFN Laboratori Nazionali di Frascati, Frascati, Italy*
[29]*INFN Sezione di Genova, Genova, Italy*
[30]*INFN Sezione di Milano, Milano, Italy*
[31]*INFN Sezione di Milano-Bicocca, Milano, Italy*
[32]*INFN Sezione di Cagliari, Monserrato, Italy*
[33]*INFN Sezione di Padova, Padova, Italy*
[34]*INFN Sezione di Perugia, Perugia, Italy*
[35]*INFN Sezione di Pisa, Pisa, Italy*
[36]*INFN Sezione di Roma La Sapienza, Roma, Italy*
[37]*INFN Sezione di Roma Tor Vergata, Roma, Italy*
[38]*Nikhef National Institute for Subatomic Physics, Amsterdam, Netherlands*
[39]*Nikhef National Institute for Subatomic Physics and VU University Amsterdam, Amsterdam, Netherlands*
[40]*AGH—University of Krakow, Faculty of Physics and Applied Computer Science, Kraków, Poland*
[41]*Henryk Niewodniczanski Institute of Nuclear Physics Polish Academy of Sciences, Kraków, Poland*
[42]*National Center for Nuclear Research (NCBJ), Warsaw, Poland*
[43]*Horia Hulubei National Institute of Physics and Nuclear Engineering, Bucharest-Magurele, Romania*
[44]*Authors affiliated with an institute formerly covered by a cooperation agreement with CERN*
[45]*Universidade da Coruña, A Coruña, Spain*
[46]*ICCUB, Universitat de Barcelona, Barcelona, Spain*
[47]*La Salle, Universitat Ramon Llull, Barcelona, Spain*
[48]*Instituto Galego de Física de Altas Enerxías (IGFAE), Universidade de Santiago de Compostela, Santiago de Compostela, Spain*
[49]*Instituto de Fisica Corpuscular, Centro Mixto Universidad de Valencia—CSIC, Valencia, Spain*
[50]*European Organization for Nuclear Research (CERN), Geneva, Switzerland*
[51]*Institute of Physics, Ecole Polytechnique Fédérale de Lausanne (EPFL), Lausanne, Switzerland*
[52]*Physik-Institut, Universität Zürich, Zürich, Switzerland*
[53]*NSC Kharkiv Institute of Physics and Technology (NSC KIPT), Kharkiv, Ukraine*
[54]*Institute for Nuclear Research of the National Academy of Sciences (KINR), Kyiv, Ukraine*
[55]*School of Physics and Astronomy, University of Birmingham, Birmingham, United Kingdom*
[56]*H.H. Wills Physics Laboratory, University of Bristol, Bristol, United Kingdom*
[57]*Cavendish Laboratory, University of Cambridge, Cambridge, United Kingdom*
[58]*Department of Physics, University of Warwick, Coventry, United Kingdom*
[59]*STFC Rutherford Appleton Laboratory, Didcot, United Kingdom*
[60]*School of Physics and Astronomy, University of Edinburgh, Edinburgh, United Kingdom*
[61]*School of Physics and Astronomy, University of Glasgow, Glasgow, United Kingdom*
[62]*Oliver Lodge Laboratory, University of Liverpool, Liverpool, United Kingdom*
[63]*Imperial College London, London, United Kingdom*
[64]*Department of Physics and Astronomy, University of Manchester, Manchester, United Kingdom*
[65]*Department of Physics, University of Oxford, Oxford, United Kingdom*
[66]*Massachusetts Institute of Technology, Cambridge, Massachusetts, USA*
[67]*University of Cincinnati, Cincinnati, Ohio, USA*
[68]*University of Maryland, College Park, Maryland, USA*
[69]*Los Alamos National Laboratory (LANL), Los Alamos, New Mexico, USA*
[70]*Syracuse University, Syracuse, New York, USA*
[71]*Pontifícia Universidade Católica do Rio de Janeiro (PUC-Rio), Rio de Janeiro, Brazil (associated with Universidade Federal do Rio de Janeiro (UFRJ), Rio de Janeiro, Brazil)*
[72]*Universidad Andres Bello, Santiago, Chile (associated with Physik-Institut, Universität Zürich, Zürich, Switzerland)*
[73]*School of Physics and Electronics, Hunan University, Changsha City, China (associated with Institute of Particle Physics, Central China Normal University, Wuhan, Hubei, China)*
[74]*Guangdong Provincial Key Laboratory of Nuclear Science, Guangdong-Hong Kong Joint Laboratory of Quantum Matter, Institute of Quantum Matter, South China Normal University, Guangzhou, China (associated with Department of Engineering Physics, Tsinghua University, Beijing, China)*

[75]*Lanzhou University, Lanzhou, China (associated with Institute of High Energy Physics (IHEP), Beijing, China)*
[76]*School of Physics and Technology, Wuhan University, Wuhan, China (associated with Department of Engineering Physics, Tsinghua University, Beijing, China)*
[77]*Henan Normal University, Xinxiang, China (associated with Institute of Particle Physics, Central China Normal University, Wuhan, Hubei, China)*
[78]*Departamento de Fisica, Universidad Nacional de Colombia, Bogota, Colombia (associated with Laboratoire de Physique Nucléaire et de Hautes Énergies (LPNHE), Sorbonne Université, CNRS/IN2P3, F-75005 Paris, France, Paris, France)*
[79]*Institute of Physics of the Czech Academy of Sciences, Prague, Czech Republic (associated with Department of Physics and Astronomy, University of Manchester, Manchester, United Kingdom)*
[80]*Ruhr Universitaet Bochum, Fakultaet für Physik und Astronomie, Bochum, Germany (associated with Fakultät Physik, Technische Universität Dortmund, Dortmund, Germany)*
[81]*Eotvos Lorand University, Budapest, Hungary (associated with European Organization for Nuclear Research (CERN), Geneva, Switzerland)*
[82]*Faculty of Physics, Vilnius University, Vilnius, Lithuania (associated with Physikalisches Institut, Albert-Ludwigs-Universität Freiburg, Freiburg, Germany)*
[83]*Van Swinderen Institute, University of Groningen, Groningen, Netherlands (associated with Nikhef National Institute for Subatomic Physics, Amsterdam, Netherlands)*
[84]*Universiteit Maastricht, Maastricht, Netherlands (associated with Nikhef National Institute for Subatomic Physics, Amsterdam, Netherlands)*
[85]*Tadeusz Kosciuszko Cracow University of Technology, Cracow, Poland (associated with Henryk Niewodniczanski Institute of Nuclear Physics Polish Academy of Sciences, Kraków, Poland)*
[86]*Department of Physics and Astronomy, Uppsala University, Uppsala, Sweden (associated with School of Physics and Astronomy, University of Glasgow, Glasgow, United Kingdom)*
[87]*Taras Schevchenko University of Kyiv, Faculty of Physics, Kyiv, Ukraine (associated with Université Paris-Saclay, CNRS/IN2P3, IJCLab, Orsay, France)*
[88]*University of Michigan, Ann Arbor, Michigan, USA (associated with Syracuse University, Syracuse, New York, USA)*
[89]*Ohio State University, Columbus, United States (associated with Los Alamos National Laboratory (LANL), Los Alamos, New Mexico, USA)*

[a]Also at Lamarr Institute for Machine Learning and Artificial Intelligence, Dortmund, Germany.
[b]Also at Università degli Studi di Milano-Bicocca, Milano, Italy.
[c]Also at Università di Roma Tor Vergata, Roma, Italy.
[d]Also at Università di Modena e Reggio Emilia, Modena, Italy.
[e]Also at Department of Physics and Astronomy, University of Victoria, Victoria, Canada.
[f]Also at Università di Ferrara, Ferrara, Italy.
[g]Also at Universidade Estadual de Campinas (UNICAMP), Campinas, Brazil.
[h]Also at Università di Bologna, Bologna, Italy.
[i]Also at Università di Genova, Genova, Italy.
[j]Also at Scuola Normale Superiore, Pisa, Italy.
[k]Also at Università degli Studi di Milano, Milano, Italy.
[l]Also at Center for High Energy Physics, Tsinghua University, Beijing, China.
[m]Also at Universidad Nacional Autónoma de Honduras, Tegucigalpa, Honduras.
[n]Also at Università di Cagliari, Cagliari, Italy.
[o]Also at Centro Federal de Educacão Tecnológica Celso Suckow da Fonseca, Rio De Janeiro, Brazil.
[p]Also at Università di Bari, Bari, Italy.
[q]Also at Università di Perugia, Perugia, Italy.
[r]Also at LIP6, Sorbonne Université, Paris, France.
[s]Also at Università di Pisa, Pisa, Italy.
[t]Also at Hangzhou Institute for Advanced Study, UCAS, Hangzhou, China.
[u]Also at Università di Padova, Padova, Italy.
[v]Also at Università di Bergamo, Bergamo, Italy.
[w]Also at Universidad de Ingeniería y Tecnología (UTEC), Lima, Peru.
[x]Also at Università di Siena, Siena, Italy.
[y]Also at Universidad de Alcalá, Alcalá de Henares, Spain.
[z]Also at Università di Urbino, Urbino, Italy.